Available online at www.sciencedirect.com
ScienceDirect
Polymer 48 (2007) 2–18
polymer
www.elsevier.com/locate/polymer

Feature Article

Deformation mechanisms in polymer fibres and nanocomposites

R.J. Young, S.J. Eichhorn*

Materials Science Centre, School of Materials, University of Manchester, Grosvenor Street, Manchester, Greater Manchester M1 7HS, UK

Received 9 October 2006; accepted 5 November 2006
Available online 4 December 2006

Abstract

This review covers the development of the understanding of the deformation micromechanics of both synthetic and natural polymeric fibres using spectroscopic and X-ray diffraction techniques. The concept of fibres as composites, where hard and stiff phases are combined with softer polymeric materials is also discussed. Starting with the first discoveries on the molecular orientation and morphology of polymeric fibres, the widely used concepts of uniform stress and strain are examined for the analysis of fibre deformation. The use of advanced techniques such as Raman and infrared spectroscopies to follow molecular deformation in both rigid-rod (*e.g.* P*p*PTA, PBO, PBT, polyethylene) and natural (*e.g.* cellulose, collagen, silk, chitin) polymer fibres is presented. A clear distinction between fibres that have structures that are subjected to uniform stress or strain is presented, with the evidence that is detected from the response of the molecules (by Raman spectroscopy) and the crystalline fraction (by X-ray diffraction). It is suggested that natural fibres, such as cellulose, silk and others, may have different types of microstructures that are subjected to a uniform strain, which could have potentially led to incorrect determinations of crystal moduli. It is also demonstrated that the Raman and X-ray techniques have been influential on our development of fibres, and have shown that the morphology plays a critical role in mechanical properties. In addition to this, the use of X-ray diffraction using microfocus synchrotron sources is also reviewed. This approach allows a more complete picture of both molecular and crystalline deformations to be developed, and with the advent of nanocomposites it is shown that a combination of the two techniques will be vital for our understanding of their exploitation in technological applications.

Keywords: Fibres; Nanocomposites; Deformation

1. Introduction

Polymer fibres and composite materials thereof have made a major contribution to the well-being and technological development of the human race. Aerospace and other advanced industries are driving the need to develop lightweight materials with high stiffnesses, strengths and fracture toughness. With these properties ultimately in mind, progress over the last 30 years into the production of high-performance polymeric fibres has been rapid. In tandem with this progress has been the development of the necessary tools to follow the deformation processes in polymeric fibres to better understand how their performance may be improved. Particular highlights have been on the development of Raman spectroscopy and X-ray (and more recently from synchrotron sources) diffraction, with which the molecular and crystal deformations of polymeric fibres can be followed in detail. Non-polymeric high-performance fibres, such as carbon-based materials, have also been studied widely using these techniques, but this article will predominantly concentrate upon the polymeric forms. The work presented has been particularly useful for studying the micromechanics of nanocomposites, which have potential as a new type of high-performance materials. A clear distinction between fibres derived by man-made routes and those of natural origin is made in terms of their structural uniform stress and strain responses to external deformation.

In this article the deformation mechanisms of polymer fibres and nanocomposites using Raman spectroscopy and X-ray diffraction, we will cover the theoretical basis for such investigations, from the early stages of inception upon synthetic fibres to more recent studies of natural polymer-based systems.

* Corresponding author. Tel.: +44 161 3065982; fax: +44 161 3063586.
E-mail address: s.j.eichhorn@manchester.ac.uk (S.J. Eichhorn).

0032-3861/$ - see front matter © 2006 Elsevier Ltd. All rights reserved.
doi:10.1016/j.polymer.2006.11.016

2. Deformation mechanisms in polymeric fibres

It has been well-known for some time that there is a good correlation between optical properties and molecular orientation in polymeric materials. Treloar first discussed the effect of the reorientation of a polymeric material (rubber), and the subsequent changes observed in birefringence measurements [1]. Later, others showed experimentally [2–4] that the optical birefringence in a wide range of polymeric materials could be used to follow the deformation of oriented chains, and could also be related to their crystalline/amorphous structure. Hermans [5] used a similar approach to these investigations for cellulose fibres, and derived orientation functions that could be obtained from simple birefringence measurements. Ward subsequently developed models [6] that interrelated structure, orientation and elastic modulus in idealised semicrystalline polymeric materials. Ward also showed in his seminal paper [6] that the relationship between mechanical anisotropy and orientation was much more complex than that between the static birefringence and orientation, and derived an expression relating the birefringence and the orientation function in a similar manner to Hermans [5]. This expression for birefringence and orientation was also confirmed experimentally for polyethylene filaments [7].

2.1. Fibre mechanics

A large number of publications, before and after these initial discoveries, dealt with the nature of the semicrystalline structure of fibres and filamentous materials, and it is beyond the scope of this review to cover this literature in full. However, it is worth mentioning the work of Halpin and Kardos [8], who for the first time gave upper and lower bands for the predictions of mechanical stiffness of semicrystalline polymeric materials based on composite theory. The lower band due to Reuss [9] assumes that the elements in the structure (*i.e.* the monomer and polymer molecules) are lined up in series and experience the same stress. The modulus of the polymer in this case, E_p will be given by an equation of the form:

$$1/E_p = V_c/E_c + (1 - V_c)/E_m \quad (1)$$

where V_c is the volume fraction of crystals and E_c and E_m are the moduli of the crystals and matrix (monomer), respectively. The second model due to Voigt [9] assumes that all the elements are lined up in parallel, and so it experiences the same strain. The modulus of the polymer for the Voigt model is given by the rule of mixtures as:

$$E_p = E_c V_c + E_m(1 - V_c) \quad (2)$$

These upper and lower bands are schematically represented in Fig. 1, where the upper band reflects a *uniform strain* structure and the lower band a *uniform stress* structure. This study by Halpin and Kardos [8] allowed the mechanical stiffness of a polymer to be derived on the basis of high and low aspect ratio crystals in an amorphous matrix, with different mechanical properties (*i.e.* high-modulus crystals and a much lower modulus matrix) without the need for the presence of tie molecules. Thermodynamic equilibrium between the crystalline and amorphous regions was assumed in their models [8], which had initially been considered as a conceptual problem with such morphologies.

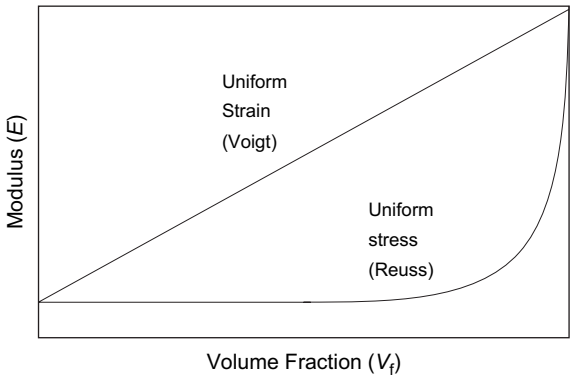

Fig. 1. The form of the upper and lower bands of modulus for uniform strain (Voigt) and stress (Reuss) models.

Aggregate models, where crystalline domains are considered in series with amorphous domains, were first derived by Ward [6], and developed later by Northolt and vanderHout [10] for highly crystalline fibres. In this series arrangement, the stress in the crystals and amorphous regions is assumed to be *uniform*. Takayanagi et al. [11] reported the use of a combined parallel-series model in which the stress in the crystals and amorphous regions is *non-uniform*, with the former overstressed and the latter understressed. In this sense, one could consider, in a fibre with such a morphology, that a stress-transfer process is taking place, and given the dimensions of the crystals, that the structure is that of a nanocomposite. Schematic diagrams of the Takayanagi model are shown in Fig. 2.

2.2. Raman spectroscopy and X-ray diffraction

To better understand the nature of local stress and its development during deformation in polymeric fibres, a number of non-contact techniques with high spatial resolution have been utilised. In this article we will focus on two such techniques; namely Raman spectroscopy and X-ray diffraction. The former is useful for determining molecular deformation and orientation, whereas the latter is sensitive to crystal and amorphous interactions. Orientation analysis, of the crystalline fraction only, is also possible using X-ray diffraction, and this will be covered in more detail later. It will be shown, however, that it is essential to use a combination of both techniques to obtain a complete understanding of the micromechanics of deformation of both semicrystalline polymeric fibres and nanocomposites.

Fig. 3a shows the Raman spectrum of a single aramid fibre obtained using a HeNe laser and Fig. 3b shows the effect of tensile stress upon the 1610 cm^{-1} Raman band. It has been established [12] that this change in Raman wavenumber, $\Delta\nu$, during the deformation of high-performance fibres is a result of chain stretching and related directly to the stress on the

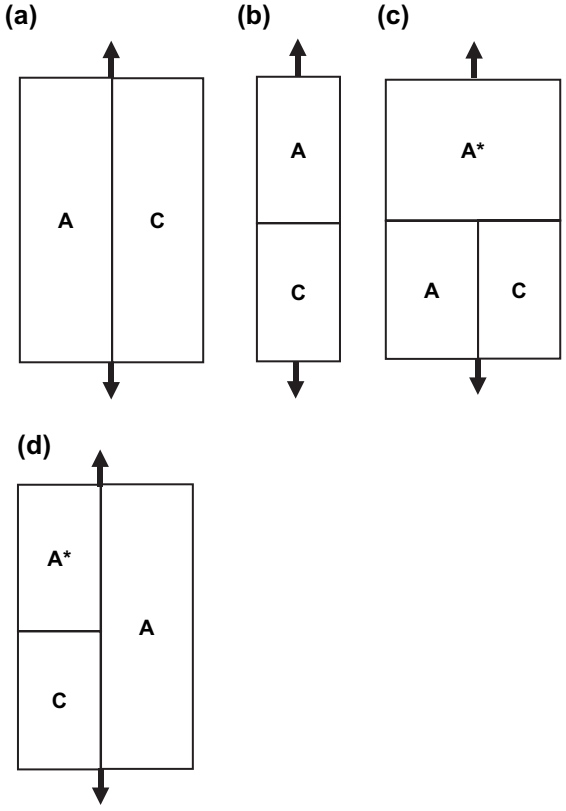

Fig. 2. Schematics of (a) a parallel, (b) a series, (c) a parallel–series and (d) a series–parallel models representative of the morphology of semicrystalline polymer fibres. A and A* are the amorphous fractions, C is the crystalline fraction and the arrows indicate the direction of applied tensile deformation.

crystalline reinforcing units, σ_r, such that for an increment of stress

$$d\Delta\nu \propto d\sigma_r \tag{3}$$

If it is assumed that the stress on the reinforcing units is the same as that on the fibre as a whole (*uniform stress*) then σ_r equals σ_f, the fibre stress, and so Eq. (3) becomes

$$\frac{d\Delta\nu}{d\varepsilon_f} \propto \frac{d\sigma_f}{d\varepsilon_f} = E_f \tag{4}$$

by dividing by an increment of fibre strain, ε_f, where E_f is the Young's modulus of the fibre. Moreover in the case of *uniform stress* since σ_r equals σ_f it follows from Eq. (3) that $d\Delta\nu/d\sigma_f$ should be independent of fibre modulus.

An alternative situation that can be employed to model the behaviour is the *uniform strain* model in which the strain on the reinforcing units, ε_r, is the same as the overall fibre strain, ε_f, which leads to

$$\frac{\sigma_r}{E_r} = \frac{\sigma_f}{E_f} \tag{5}$$

where E_r is the Young's modulus of the reinforcing units. Rearranging and using Eq. (3) gives

$$\frac{d\Delta\nu}{d\sigma_f} \propto \frac{E_r}{E_f} \tag{6}$$

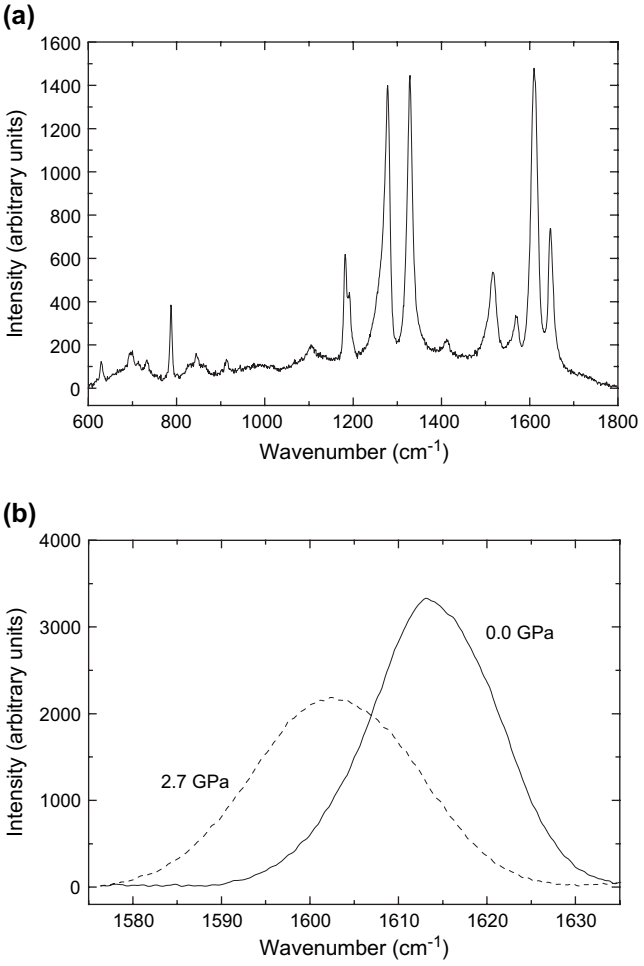

Fig. 3. (a) Raman spectrum obtained from a single aramid polymer fibre. (b) Shift of the 1610 cm^{-1} Raman band with tensile stress (data replotted from Ref. [12]).

Since it can assumed that the modulus of the reinforcement, E_r, is constant then

$$\frac{d\Delta\nu}{d\sigma_f} \propto \frac{1}{E_f} \tag{7}$$

Hence it is predicted that in the situation where there is a *uniform strain* in the fibre, $d\Delta\nu/d\sigma_f$ should be proportional to the reciprocal of the fibre modulus, $1/E_f$. If the band shift is measured as a function of strain then using Eq. (3) and since the strain is uniform

$$\frac{d\Delta\nu}{d\varepsilon_f} = \frac{d\sigma_r}{d\varepsilon_r} = E_r \tag{8}$$

Hence since E_r is constant, then $d\Delta\nu/d\varepsilon_f$ is constant. The results of these predictions for Raman band shifts in the cases of uniform stress and uniform strain are summarised in Table 1.

It is possible to make an analogous set of predictions for experiments upon the deformation of polymer fibres using X-ray diffraction. Fig. 4a shows a wide-angle X-ray diffraction pattern obtained from a single PBO high-modulus polymer fibre and Fig. 4b shows the shift of the (005) and (006) layers that lie in a fibre subjected to tensile deformation. In this

Table 1
Predicted dependence of the Raman band shift rates with both strain and stress for the different models of fibre structure

Band shift	Uniform stress	Uniform strain
$d\Delta\nu/d\varepsilon_f$	$\propto E_f$	Independent of E_f
$d\Delta\nu/d\sigma_f$	Independent of E_f	$\propto(1/E_f)$

Table 2
Predicted dependence of the crystal strain determined using X-ray diffraction upon both strain and stress for the different models of fibre structure

Crystal strain	Uniform stress	Uniform strain
$d\varepsilon_c/d\varepsilon_f$	$\propto E_f$	Independent of E_f
$d\varepsilon_c/d\sigma_f$	Independent of E_f	$\propto(1/E_f)$

case the shift of the layer lines towards the main beam indicates that the lattice parameter in the chain direction, c, increases on the application of a tensile stress. The crystal strain ε_c is defined as $\Delta c/c$, and assuming that the crystals are the reinforcing units in the structure, and they undergo elastic deformation, it follows that for an increment of stress

$$d\varepsilon_c \propto d\sigma_r \tag{9}$$

This relationship is analogous to Eq. (3), and so it is possible to make a similar set of predictions for the variations of $d\varepsilon_c/d\varepsilon_f$ and $d\varepsilon_c/d\sigma_f$ with fibre modulus, and E_f for the situation of uniform stress and uniform strain. These predictions are shown in Table 2. It should be noted that $d\varepsilon_c/d\varepsilon_f$ is not usually measured for a fibre but the reciprocal of $d\varepsilon_c/d\sigma_f$ is normally determined, and a uniform stress assumption made. It is then termed the crystal modulus, $E_c = d\sigma_f/d\varepsilon_c$.

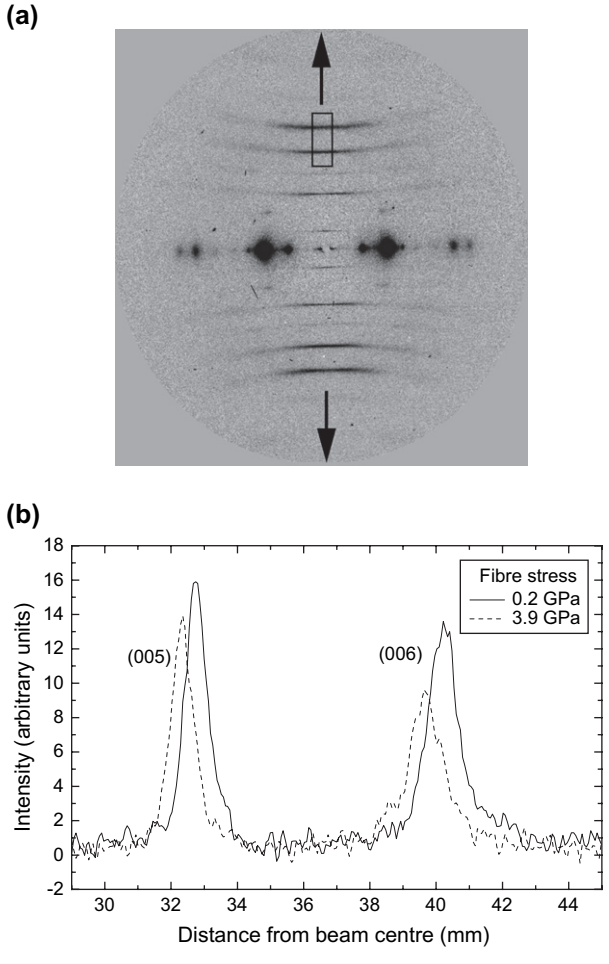

Fig. 4. (a) Synchrotron microfocus X-ray diffraction pattern obtained from a single poly(*p*-phenylene benzobisoxazole) PBO fibre. (b) Shift of the (005) and (006) Bragg peaks (outlined in the box in (a)) with tensile stress applied along the fibre axis (data supplied by Dr. Richard Davies). Arrows indicate the direction of fibre stress although the layer line reflections themselves move closer to the centre of the diffraction pattern under tensile stress.

3. Raman spectroscopy and molecular deformation

The Raman effect was first discovered by the distinguished Indian scientist, Chandrasekhara Venkata Raman in 1924 [13]. The secondary radiation that was observed in his experiments was a consequence of inelastic scattering of light by the molecules [14]. In the early developmental stages of Raman spectroscopy, because of low intensity sources of radiation compared to the modern laser systems, and because the effect itself is very weak, infrared spectroscopy of polymers was far more popular as a technique of choice for the characterisation of polymers [15–19]. However, even in these early stages of development, Raman spectra were reported from polymeric materials such as polystyrene [20]. Until the development of laser technology, and particularly the emergence of new optical rejection filters [21] for enhancing Raman Stokes and anti-Stokes spectral peaks, and the microscope or microprobe system for high spatial resolution [22], detailed studies of polymers were not possible. Interest then began into using vibrational spectroscopy to follow local changes in the structure of polymer fibres. Further interest in the use of Raman spectroscopy to characterise polymers has increased with the development of polymers with conjugated backbones which undergo resonance Raman scattering and give strong, very well-defined spectra. After the initial studies on the characterisation of static samples, people began to use these techniques to understand deformation processes and the progress of this work will now be reviewed.

3.1. Background and theory

Perhaps the predecessor for the observations of shifts in the positions of Raman bands of high polymer fibres was the discovery of a similar effect using infrared spectroscopy [23–26]. It became clear during the early 1970s that orientation changes in polymeric materials could be followed using infrared and *in situ* deformation [27]. In addition, and during the same period, Wool showed that the intensity maxima in number of polymers shifted towards a lower wavenumber upon external deformation [28,29]. Initially Zhurkov et al. proposed that the rate of the shifts of different bands with strain within a polymeric material was constant [23]. However, Wool showed that this was not true, and that this factor depended on the ‘‘molecular stress distribution via the morphology of

the sample'' [29], which is a point which will be addressed at the later stage in this article.

In 1977 Mitra et al. [30] made the discovery that when conjugated polydiacetylene single crystal fibres were deformed in tension, Raman bands located at 1498 cm^{-1} (corresponding to the −C═C− backbone moiety) and 2104 cm^{-1} (corresponding to the −C≡C− backbone moiety) shifted the position towards a lower wavenumber [30]. The shifts are shown in Fig. 5 [30]. This effect was also predicted theoretically [30] by using an analysis based on anharmonic force constants of bonds within an idealised polymeric chain and Badger's rule [31], which interrelates the force-constant with the equilibrium separation of neighbouring atoms [31]. In this sense, Mitra et al. [30] showed that the shift was due to direct stretching of the polydiacetylene polymer backbone, and the subsequent change therefore in the force constants of the bond was associated with this structural form. This was argued over the counter explanations of changes in the local refractive index of matrix material surrounding a chain, which would also result in decreased delocalisation and potentially in a band shift [30]. Batchelder and Bloor also predicted the band shifts in polydiacetylene based on a model of point masses and anharmonic spring constants [32].

Previous studies on the plastic deformation of crystals of bis(*p*-toluene sulfonate) 2,4-hexadiene-1,6-diol (TSHD) had shown that the predominant stress-relieving process in such materials was a twinning or kinking of the polymer chains [33]. However, since this would not occur in tension, it was assumed by Batchelder and Bloor [32] that polydiacetylene single crystals could in theory sustain large tensile stresses along their backbones without the occurrence of plastic deformation [32]. It is worth noting at this point that Raman spectroscopic studies of the molecular deformation of all types of polydiacetylene single crystals reveal that the band shift rate per unit strain $d\Delta\nu/d\varepsilon_f$ is invariant ($\sim 20\ cm^{-1}\%^{-1}$), irrespective of the side groups that are present along the main chain [34].

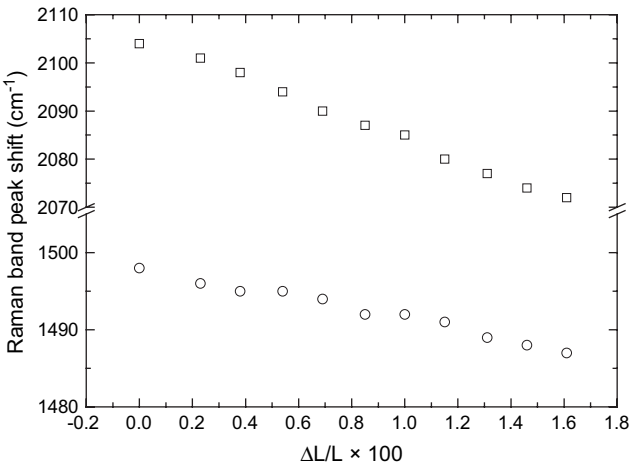

Fig. 5. Raman band shifts as a function of applied tensile strain for two Raman bands for polydiacetylene single crystals (key: □ − 2104 cm^{-1} and ○ − 1498 cm^{-1} Raman bands corresponding to −C≡C− and −C═C− moieties respectively; data replotted from Ref. [30]).

The polydiacetylene crystal or fibre modulus is controlled by the size of these side groups, and this observation that $d\Delta\nu/d\varepsilon_f$ is independent of E_f means that, with reference to Table 1, the reinforcing units (the polydiacetylene backbones) are subjected to the same strain as the fibre as a whole (*i.e. uniform strain*).

Inspired by these observations upon polydiacetylene single crystals, initial attempts to follow band shifts in rigid-rod polymers, such as Kevlar, were, however, unsuccessful, and the lack of an effect was put down to only a small part of the structure being under sufficient stress [35]. In 1985 band shifts were observed for the first time in stressed Kevlar fibres [36], and after some initial evidence to the contrary [37] it has been shown conclusively that this method is viable for determining local deformation provided that precautions to avoid radiation damage (*e.g.* the choice of laser type and power) are taken into account [38].

3.2. Characterisation of synthetic polymeric fibres

After the initial studies on diacetylenes, Raman band shifts in high-performance polymer fibres such as poly(*p*-phenylene benzobisthiazole) (PBT) fibres were reported [39], although infrared band shifts had already been observed for these materials [40]. Significant breakthroughs were then made in obtaining morphological information from stressed polymers, the most notable around this time being the work of Grubb and Prasad on high-modulus polyethylene fibres [41]. Band shifts were not only observed for the 1063 cm^{-1} peak, corresponding to the C−C asymmetric stretch mode, but also observed to broaden asymmetrically, which was something not seen for the X-ray diffraction layer lines for the same material under tensile deformation. This asymmetric broadening was attributed to 'taut-tie' molecules within the amorphous regions of the fibres, and it was found to be only a partially reversible effect, with relaxation occurring over time. The crystals were found to go into compression when the load was removed from the fibres, suggesting that the relaxation of the taut-tie chains was slow. Ultra-high molecular weight gel-spun fibres were also investigated using the same techniques by another research group [42]. A later paper [43] found that 40% of the Raman-active crystalline phase was subjected to high strain and the mechanisms and morphology proposed were different to those of Grubb and Prasad [41].

Perhaps the most important contribution to understand the deformation of polymeric fibres using Raman spectroscopy was from a series of papers on rigid-rod materials; namely P*p*PTA, PIPD and others [39,43,44]. The first of these studies detailed only PBT and PBO [39,43] but a later paper outlined molecular deformation in more detail for poly-aromatic rigid-rod fibres [44]. This paper [44] showed that for a range of different fibres (Kevlar, Twaron, Technora, PBO, PET) the stress-induced Raman band shift for the 1610 cm^{-1} peak, corresponding to the aromatic ring stretch was invariant and equal to a value of roughly $-4.0\ cm^{-1}$/GPa (shown in Fig. 6a for Kevlar fibres [44]), although the band shift rates per unit strain were reported to vary (shown in Fig. 6b for Kevlar fibres [44]).

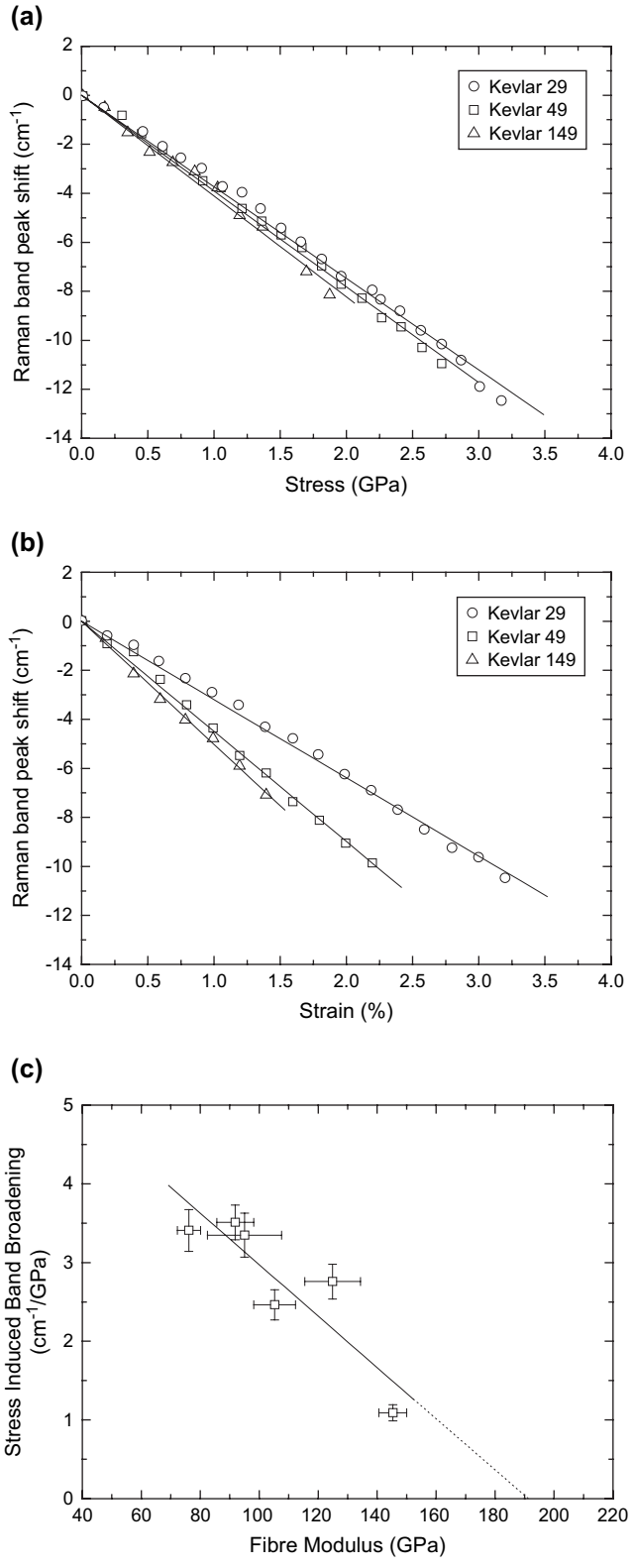

Fig. 6. Raman band shifts as a function of (a) tensile stress, (b) tensile strain for a range of Kevlar fibres (29, 49 and 149); (c) Stress-induced Raman band broadening as a function of fibre modulus for a range of Kevlar and Twaron fibres (data replotted from Ref. [44]. Original data [44] was not fitted with an error weighted linear line. If this is done then the predicted modulus is reduced to 180 GPa).

This result was in spite of the fact that some of the fibres had different chemical structures and were produced using different procedures resulting in different microstructural morphologies. Stress-induced band broadening was also reported for all fibres (Fig. 6c reports this result for Kevlar fibres [44]), which was shown to decrease with increasing fibre modulus for the P*p*PTA (Kevlar and Twaron) fibres, approaching zero for a fully crystalline structure. Symmetrical broadening of the 1610 cm^{-1} peak was reported for Kevlar, Twaron, Technora and PBO fibres, whereas PET showed asymmetric broadening. This difference was reported to be due to the fact that some of the bonds in PET must be overstressed, as had been detailed previously [45].

Finally, the deformation of all fibres was shown to follow the continuous chain model of Northolt et al. [46] wherein the structure deforms by a chain extension, orientation and sequential plastic deformation due to shear between the crystallites. This model is similar to an approach by Davies et al. [47] who showed that a number of thermotropic liquid crystalline polyesters and polyamides deformed by this mechanism. One outcome of this type of deformation is the increase in the fibre modulus as the deformation proceeds into the high strain region [46,47], which was seen for all the rigid-rod fibre samples analysed by Young and Yeh [44]. This type of strain stiffening has been seen more clearly from the molecular deformation of a number of cellulose fibres by Kong and Eichhorn [48]. The molecular deformation in PBO fibres was also reported [49,50] wherein it was shown for a range of fibres (AS, HM and HM+) that band shifts in the 1618 cm^{-1} band, corresponding to the aromatic stretch, could be used for this purpose. It was also found [49] that reduced changes in the FWHM (full-width-half-maximum) of the 1618 cm^{-1} peak for HM+ fibres could be accounted for due to their more homogenous structure. A second paper in this series [50] showed that less hysteresis in the HM+ fibres supported this hypothesis. Skin–core orientations were also inferred from the distributions of the radial 2θ intensity profiles by SAED (Selective Area Electron Diffraction) where the core of the fibres was found to be less oriented than the skin. This type of skin–core orientation had been previously reported for P*p*PTA fibres [51] where it was shown that different Raman band shift rates could be obtained from fibres with different skin orientations as the Raman signal is recorded only from this region of the fibres.

Galiotis et al. in a recent paper [52] have reported a more detailed description of the effect of stress dependent shifts of two Raman optical phonons ($\nu_1 = 1611\ cm^{-1}$ and $\nu_2 = 1648\ cm^{-1}$) for P*p*PTA fibres at different temperatures. The fibres were deformed inside a furnace, and spectra were recorded under isothermal conditions. It was found that ν_1 was moderately anharmonic and ν_2 was harmonic and that both soften with axial deformation, under isothermal conditions, irrespective of the fibre modulus. However, under increased temperatures (above 25 °C) the phonons appeared to harden. This result was also predicted, based on a theoretical approach that treats the fibres as molecular wires with negative expansion coefficients. This paper [52] represents the first

study of molecular deformation using Raman spectroscopy with environmental control.

3.3. Characterisation of natural polymeric fibres

Raman and infrared spectroscopic characterisations of natural fibres in recent times have developed into an area that is gaining interest worldwide. It must be noted, however, at this point that spectroscopic characterisation of natural materials is fraught with difficulty. It is found that light scattering from such samples is often not very intense and they sometimes undergo fluorescence, and hence longer exposure times are required if one is to obtain well-resolved Raman spectra. Resonance Raman also does not occur for natural polymers such as cellulose, and hence the high intensities seen in polymers such as the diacetylenes are not possible. Nevertheless there have been developments in laser technology that have led to the availability of high-power near infrared lasers that significantly reduce fluorescence.

One of the first reported Raman (and infrared) studies on undeformed plant materials (cellulose) was the work by Blackwell et al. in the early 1970s [53]. Since 1940s people had been using infrared spectroscopy to conduct structural characterisations of hydrogen bonding in plant based cellulose [54]. It is interesting to note that even at this very early stage, Ellis and Bath [54] were able to see changes in the hydrogen bond system of the cellulose structure before and after chemical treatment. After this initial period, a number of detailed papers were published on using infrared spectroscopy for structural characterisation of celluloses by Marchessault and Liang [55–57].

Blackwell et al. [53] obtained Raman and infrared spectra from the cell walls of the algae *Valonia ventricosa* using an argon ion laser and a Spex-1400 double monochromator, and assigned a number of bands to particular parts of the structure. Later on in 1970s Koenig and Lin also reported Raman spectra for silk, wool, hair and feather [58]. A great deal of effort was made during 1970s by Atalla and Wiley to use Raman spectroscopy to characterise cellulosics, most of which has been extensively reviewed elsewhere [59]. Equipment in those days was reliant on photomultiplier tubes for recording the spectra, but the development of CCD (charge-coupled devices) for recording signals from spectrometers has greatly reduced exposure times [60]. Finally, perhaps the most important part of work on the characterisation of natural fibres has been the work of Edwards et al., including detailed band assignments of cellulosics [61], silks [62], wool [63] and hair [64]. However, it was only in the late 1990s people began to look at the deformation of natural fibres using spectroscopic techniques.

The first study on the molecular deformation of cellulose fibres using Raman spectroscopy was on regenerated forms by Hamad and Eichhorn [65]. This showed for the first time that band shifts, as reported for synthetic fibres, were observable for cellulosic materials. However, there were problems in resolving the shifts with lower modulus fibres, and indeed this study [65] showed that larger band shifts per percent tensile strain applied could be obtained with stiffer fibres. This was indeed achieved with natural plant fibres (flax and hemp) a few years later [66] (Fig. 7) and it was shown that the rate of band shift with respect to strain was directly proportional to the stiffness of the fibres. More studies on these effects were then followed [67,68] to investigate the deformation of wood and other plant fibres in detail. In recent times these types of experiments have been repeated by two independent groups at the University of Halle and at the Max Planck Institute [69–71]. The first of these studies showed that it was indeed possible to detect band shifts in plant material with different chemical and enzymatic treatments [70]. Unlike the original work by Eichhorn et al. [66,67] it was not necessary to pre-bleach the fibres using hydrogen peroxide to overcome problems with fluorescence, as an FT (Fourier Transform) Raman system was used.

Other studies on the deformation micromechanics of cellulose fibres have used infrared spectroscopy. Of particular note has been the work of Salmén and co-workers on the use of dynamic infrared spectroscopy to elucidate the complex hydrogen bond interactions during the loading of the cellulosic chains during deformation [72,73]. Without recourse to a full review of the area, the role of the –OH moiety in cellulose spectra is notoriously difficult to interpret. We now know, from detailed studies on the structure of cellulose polymorphs [74–77], that the disorder along the chains and the interdigitation of disorder may play a key-role in mechanics and structural interconversion [78], and hence our understanding of the mechanics of this aspect of the structure is vital. Indirect evidence of the breakdown in hydrogen bonding has recently been obtained from Raman spectroscopic studies of deformed cellulose-II fibres [48], but it is difficult to ascertain within which part of the structure (crystalline or amorphous) this is occurring [48]. However, distinct plateaus in the band shift were observed for both the 1095 cm^{-1} and 1414 cm^{-1} bands of fibres produced using different draw ratios (Fig. 8), which was attributed to a breakdown in the hydrogen bonding.

Some work has been reported on the use of Raman spectroscopy to probe the deformation of collagen (in the

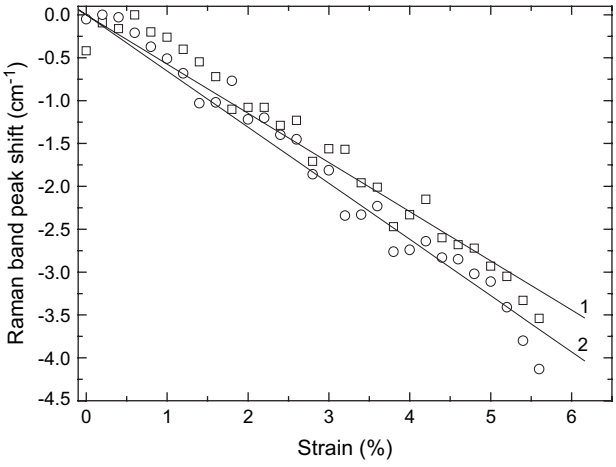

Fig. 7. Raman band shifts from the maximum for a flax fibre. 1 – 1122 cm^{-1} peak and 2 – 1095 cm^{-1} peak [66] (data replotted from Ref. [66]).

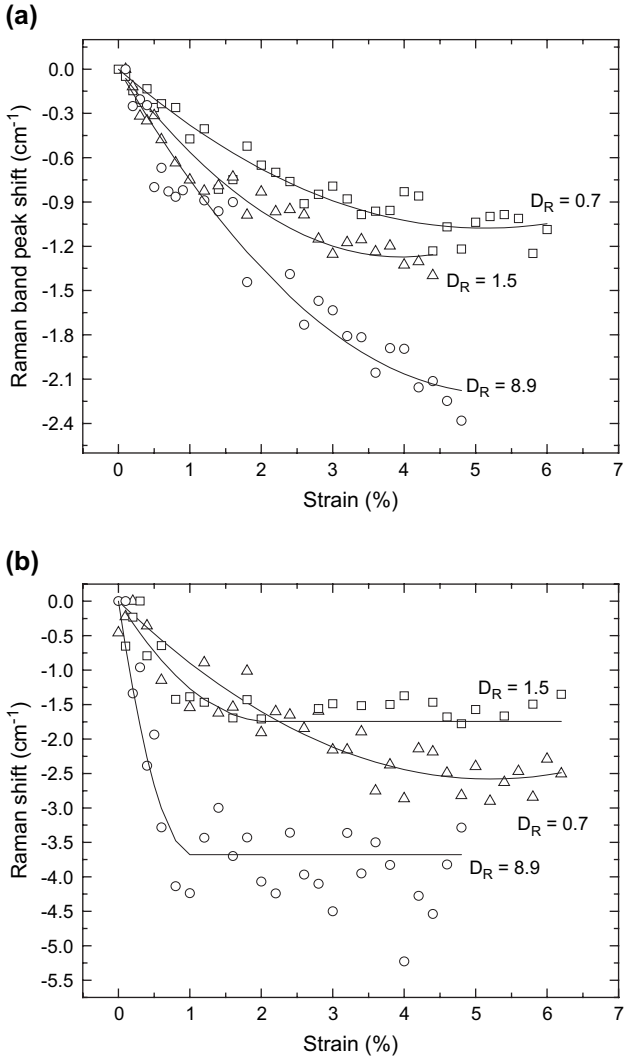

Fig. 8. Raman band shifts of the (a) 1095 cm^{-1} and (b) 1414 cm^{-1} peaks as a function of applied strain for regenerated cellulose fibres produced using a range of draw ratios ($D_R = 0.7$, 1.5 and 8.9) (data replotted from Ref. [48]).

dry-state) [79] and silk [80,81]. The work on collagen fibres [79] showed that it is possible to obtain Raman band shifts, and therefore indications of molecular deformation. However, the deformation on silk, using both silkworm and spider forms of the material, reported that the structure responded in a near uniform stress fashion. The exact conformational structure of silk fibres is still in debate, but most people accept that there are β-pleated sheets (hard segments) within an entangled amorphous network (soft segments) as originally suggested by Termonia [82]. This structure has been confirmed by others in light of further experimental evidence [83,84]. The exact location of the amorphous segments relative to the crystalline β-pleated sheet segments will determine whether the material undergoes uniform stress or strain deformation, but Termonia's model [82] would appear to be a uniform strain structure.

Various attempts to understand the morphology of silk have been made, starting with modelling of the chain stiffness. The chain stiffness of an alanine–glycine di-peptide structure has been found to be ~135 GPa [85]. In spite of this, experimental determinations of the crystal modulus have been comparatively lower in magnitude (in the range 20–28 GPa) [86,87]. The deficiency of the uniform stress assumption for silk fibres has in fact been recently highlighted [86], where it was found that the crystal modulus varied as a function of the crystallinity for a range of fibres (Fig. 9). The values of crystal modulus reported in this study [86] are apparently comparable with theoretical values when using seemingly improved computational analysis, and the acknowledgement of relaxation of the fibre stress is taken into account [88]. However, differences could still be due to the fact that there is *an inherent assumption that the structure is subjected to a uniform stress* during the measurement of crystal modulus. If this were not true, and the structure was more akin to a nanocomposite, subjected to uniform strain, then one might expect that the crystals would be overstressed, with an understressed matrix component. This has recently been experimentally proven for silk fibres [89], and some evidence for this type of microstructure has also been found in cellulose-II fibres [90]. The work recently reported for silk fibres [89] showed that the Raman band shifts as a function of stress ($d\Delta\nu/d\sigma_f$) are proportional to the inverse of the fibre modulus ($1/E_f$), *i.e.* conforming with the uniform strain model (Table 1). This result is in direct contrast to the rigid-rod polymer fibres where there is a proportionality of $d\Delta\nu/d\varepsilon_f$ with the modulus E_f [for instance Ref. [45]], *i.e.* uniform stress model (Table 1).

3.4. Modelling stress-induced Raman band shifts in polymeric fibres

Perhaps, the first attempt to explain a Raman band shift in theoretical terms was made by Mitra et al. [30] who gave an empirical relationship for the effect based on anharmonic potentials, and predicted that the shifts were seen in polydiacetylene single crystal fibres (Fig. 5). Important work has been undertaken by Tashiro [88] upon the prediction of spectroscopic (particularly Raman) band shifts, including work

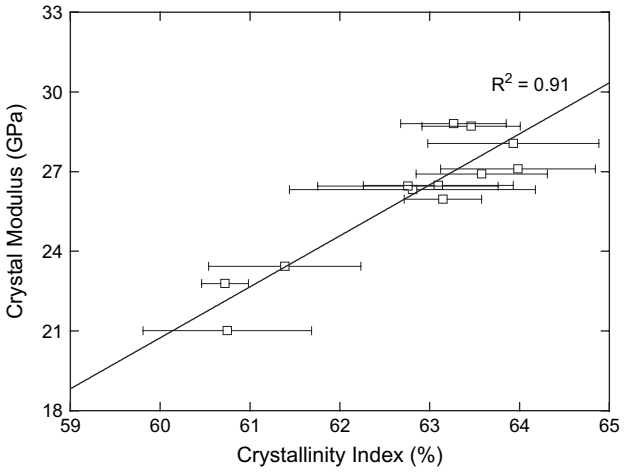

Fig. 9. Crystal modulus as a function of crystallinity for a range of fibres along the length of the cocoon of the *B. mori* silkworm (data replotted from Ref. [86]).

upon POM (polyoxymethylene) and PE (polyethylene) chains. Using general expressions for the strain energy and potential functions of asymmetric and symmetric vibrations, Tashiro [88] was able to obtain good predictions for the rate of his experimentally determined Raman band shifts. This type of approach was later applied to a PBO chain by Kitagawa et al. [91] and more rigorously for the case of a semicrystalline structure [92].

Now, this approach is adequate in the case where non-bonded interactions do not significantly contribute towards the deformation of the structure. However, little or no work exists on modelling Raman band shifts using molecular force fields. This type of approach uses a normal mode analysis to predict vibrations of minimised structures. Normal mode analyses on static theoretical cellulose structures have been previously performed [93], but not for deformed polymer chains. In recent times Eichhorn and others [90,94] have used a commercial force field, a molecular mechanics approach and normal mode analysis to predict band shifts in cellulose polymorphs (both I and II). Each structure was taken from recently published atomic coordinates [74–76] and minimised within a commercial force field (COMPASS™) under restraint. The normal mode analysis used predicted infrared intensities, and by a process of elimination a number of bands were chosen which best represented the experimentally observed Raman band shifts. Good agreement with the experimental data was obtained, and also with chain stiffness data obtained from X-ray diffraction, a subject to which we will turn to now.

4. X-ray diffraction and crystal deformation

The development of high-performance polymer fibres relies on the ability to maximise the influence of the mechanical properties on the stiff crystals that reinforce them. In a semicrystalline polymer this is never easy, due to misorientation and the effects of the amorphous regions. However, to obtain a theoretical upper limit to the mechanical properties achievable from such fibres, it has been a goal to determine, either by theoretical or experimental means, the inherent stiffness of the crystalline component. So far we have discussed the use of spectroscopic methods, which by their very nature obtain information from both the crystalline and amorphous regions. Therefore, the use of techniques such as X-ray diffraction and modelling has enabled a better picture of crystalline deformation to be obtained.

4.1. Background and theory

One of the earliest studies on the prediction of the stiffness of a polymeric chain was that of Meyer and Lotmar in 1936 [95] on cellulose. This theoretical treatment relied on primitive X-ray diffraction determinations of the structure of native cellulose from ramie fibres [96], and an assumption of a pyranose ring structure for the anhydroglucose units. Nevertheless, values of around 130 GPa were obtained using a classical mechanical approach for the deformation relying on chain stretching and rotation of bonds. Subsequent spectroscopic information allowed Lyons [97] to approach this determination with better precision, but due to an error in his calculation he obtained an overestimated value. This was corrected by Treloar [98] through an alteration in the angle bending stiffness calculations, but his value of 56 GPa was subsequently found to be too low, probably due to a lack of hydrogen bonding in his structure. Treloar also studied other polymers such as polyethylene and nylon [99] and PET [100]. Prompted by Treloar's efforts, Mann and Roldan-Gonzalez [101] in 1962 measured the crystal modulus of cellulose by deforming Fortisan (cellulose-II) fibre bundles and determined the percentage changes in the crystal strain from shifts in the 040 Bragg reflections. Sakurada et al. simultaneously published a classic paper where they measured, using X-ray diffraction on bundles of fibres held under constant stress, the elastic moduli of crystalline regions of polyethylene, poly(vinyl alcohol), polypropylene, polyoxymethylene and cellulose [102] *by assuming a uniform stress response of the structure to applied deformation* (Table 2). Examples of the crystal deformation of polyoxymethylene and cellulose are reported in Fig. 10 [102]. Subsequently,

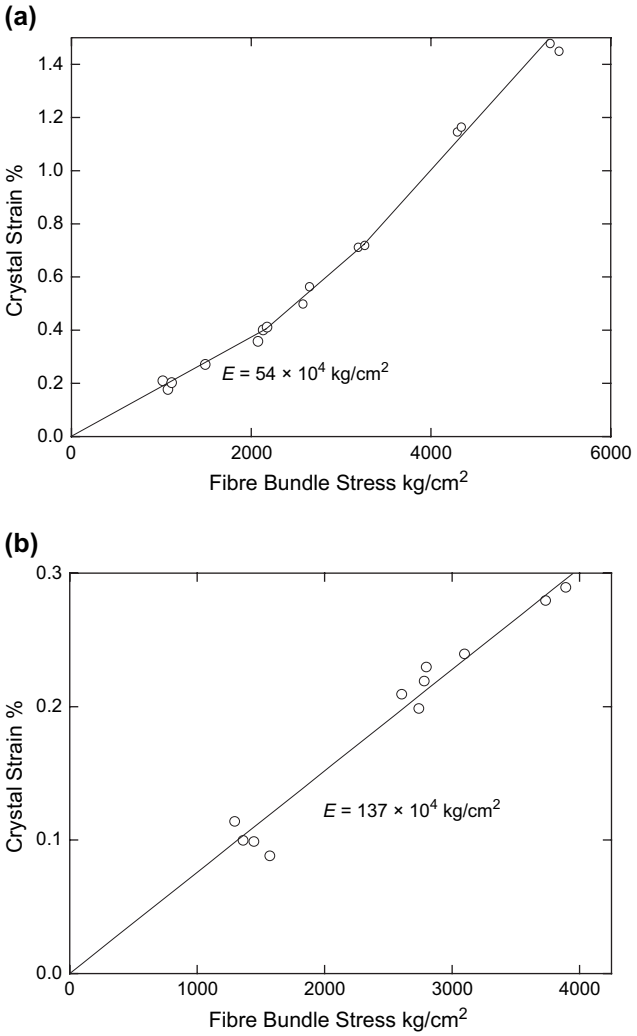

Fig. 10. Stress–strain curves for (a) polyoxymethylene and (b) cellulose obtained by X-ray diffraction and fibre bundle deformation (data replotted from Ref. [102]).

people were then able, from macromechanical tensile measurements and more detailed diffraction studies, to suggest chain-folded structures for polymer fibres [103]. Such folded structures and a full review of the development of morphological studies of this kind are somewhat beyond the scope of this article. However, it is worth noting that this type of structure was refuted strongly for cellulose [104], with some of the arguments against such morphologies being based on the work of Sakurada et al. [102]. This despite initial experimental evidence being in favour of a chain-folded structure [105]. However, a chain-folded structure could be considered to be a fully uniform strain type morphology, and it is clear that this is not always the case, with a possible hybrid model best explaining mechanical properties [90].

4.2. Crystal deformation in synthetic polymeric fibres

During the mid-to-late 1970s people began to develop oriented fibres, of which some, such as aromatic polyesters, were investigated in terms of their crystal response to deformation using X-ray diffraction [106]. With the advent of high-performance fibres, the so-called "rigid-rod" polymers, such as Kevlar [107], new studies on their properties and potential as reinforcements in composites, amongst other applications, were published. The first such study on the crystal structure of Kevlar or poly(*p*-phenylene terephthalamide) (P*p*PTA) fibres was reported by Northolt and vanAarts in 1973 [108], although this has recently been refined using neutron diffraction [109]. Subsequently, Northolt went on to elaborate in more detail the mechanical response of highly oriented P*p*PTA fibres relating crystal modulus and the orientation parameter of misoriented crystals in a formal manner [110] by equation

$$\frac{1}{E_f} = \frac{1}{E_c} + \frac{\langle \sin^2 \theta \rangle}{2g} \tag{10}$$

where E_f is the fibre modulus, E_c is the crystal modulus, $<\sin^2 \theta>$ is the crystal orientation and g is the shear modulus. Northolt [110] plotted the reciprocal of the dynamic fibre modulus against changes in orientation (determined by X-ray diffraction) for a number of deformed P*p*PTA fibres to show that this relationship was followed (Fig. 11). Subsequent deformation cycles also showed that the uniform stress model was consistent for these types of fibres.

Another notable study on these fibres was a measurement of the crystal moduli of Kevlar 49, 29, HM-50, Ekonol, Vectran and PEEK (poly(ether ether ketone)) fibres parallel to their axes [111]. For the first time the relationship between fibre properties and crystal modulus was reported [111].

Perhaps the most notable addition to the family of rigid-rod fibres has been the development of the poly(*p*-phenylene benzobisoxazole) (PBO) types; commercialised as Zylon™ by Toyobo, Japan. The structure was first synthesised by Wolfe and others as part of the US Air Force research programme into high-performance rigid-rod fibres [112]. One of the first publications to appear on the structure and morphology of PBO fibres was by Krause et al. [113]. They used wide-angle

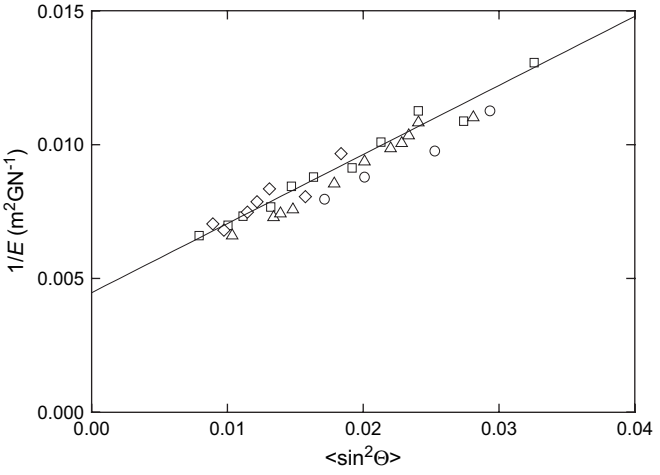

Fig. 11. The reciprocal of the dynamic compliance as a function of the orientation parameter $<\sin^2 \theta>$ for a range of P*p*PTA fibres during deformation. The data showed accordance with Eq. (10) and hence a series aggregate model appropriately describes the relationship between their mechanical properties and structure (data replotted from Ref. [110]).

X-ray analysis and high-resolution electron microscopy to study the morphology, and reported a modulus of 370 GPa for the fibres compared to 132 GPa for P*p*PTA. A few years later Martin and Thomas used X-ray diffraction techniques to obtain unit cell dimensions and HRTEM (high-resolution transmission electron microscopy) and SAED (selected area electron diffraction) to obtain lateral spacings between molecules [114]. They were also able to image and characterise defects in the fibres and show that they were edge dislocations. More detailed analyses of the packing disorder, using X-ray imaging and computer simulation, were subsequently reported by Tashiro et al. [115], and in a similar manner to Northolt's treatment of P*p*PTA fibres [110], a crystal modulus was estimated to be 370 GPa. This value was later found to be similar to an experimental value (372 GPa) determined by X-ray diffraction of three different forms of PBO fibre bundles [116].

However, the most recent development in the analysis of the crystal moduli of rigid-rod polymeric fibres using X-ray diffraction has been the development of microfocus beamlines, one of which has been at the ESRF (European Synchrotron Radiation Facility) in Grenoble [117]. This development has enabled, for the first time, the determination of crystal moduli of single filaments of high-performance fibres, the first of which to be reported was P*p*PTA [118]. Single fibres are perceived to be better for such studies, than bundles say for instance, because for the latter, average measurements have to be taken over a larger number of fibres. It is also hard to apply high uniform strains to bundles of fibres, and this could be quite critical if one were attempting to differentiate between uniform stress and strain situations. Following this, a series of papers were published by Davies and co-workers [119–124] using this beamline to study in detail the crystalline deformation and texture analysis of three forms of PBO fibre; namely AS (as-spun), HM (high modulus) and HM+ (an advanced form of HM). The first of these papers [119] showed

that the crystal moduli of the AS and HM+ fibres were very similar (on an average ~450 GPa) and the HM sample showed the highest overall value of this parameter. Raman spectroscopy was also used to follow the molecular deformation of the fibres and it was shown that a direct proportionality between band shift rate with strain and fibre modulus exists (Table 1), in agreement with a uniform stress model (see Fig. 12). A later paper [120] compared the crystal moduli of PBO fibres to that of PBT and PIPD (initially commercialised as M5 fibres by Magellan and subsequently in partnership with DuPont Advanced Fibre Systems). Similar crystal moduli for PBO and PIPD were obtained (~440 GPa) but PBT was found to have a much lower value of this parameter (350 GPa). This difference was attributed to the non-linearity of the PBT monomers in the unit cell, and demonstrated the superior properties of PBO, and the benefit of post heat treatment during processing.

The use of a micron-sized beam allows the crystal strain and skin–core orientation of fibres to be mapped spatially across their diameter, and this has been done in some detail using the facility at the ESRF. In one particular study on PBO fibres [121] it was shown that the distribution of crystal strain was uniform across the HM form of the filaments. This study also reported the onset of reorientation across an AS fibre, and showed that this form of deformation mechanism was more significant compared to what was seen for HM and HM+ fibres. This suggested that the uniquely high initial crystal orientation of HM and HM+ fibres contributed to their superior mechanical properties compared to AS fibres. Subsequent experiments also looked at cyclic studies on AS, HM and HM+ fibres and in addition to previous studies, the transverse changes in unit cell parameters [122]. The unit cell angle was found to increase, and the unit cell volume change was found to be invariant for all fibre types. For HM+ fibres the changes in *c*-spacing were comparatively larger than for HM fibres, hence the lower crystal modulus. These changes were however due, for HM+ fibres, to volume change invariance compensated by changes in the *a* and *b* cell dimensions. This result confirmed why differences were seen between the fibre types [123]. A major advance in thinking regarding radial fibrillar texturing (RFT) and fibre homogeneity was then reported [123]. This study showed that by using the FWHM (full-width-half-maximum) of equatorial peaks, and an assumption of the *a*-axes oriented radially about the fibre axis, one could show that the degree or distribution of RFT was directly related to fibre modulus. Heat treatment was shown to reduce this distribution. By plotting the FWHM distribution against fibre modulus it was shown that a closer estimation (~470 GPa) of crystal modulus was obtained then by the Northolt approach [110,115].

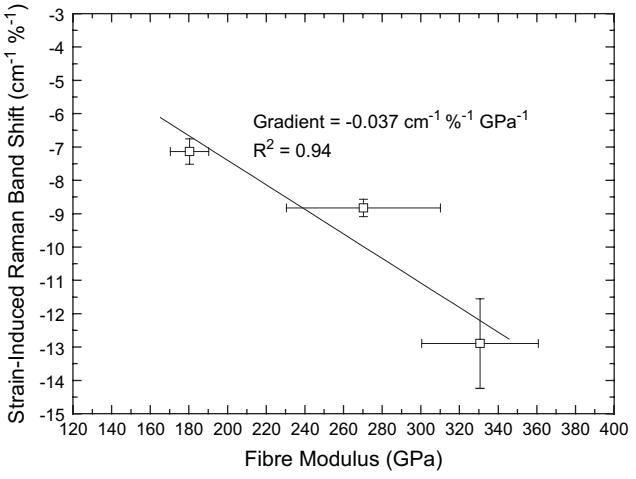

Fig. 12. Strain-induced Raman band shift as a function of fibre modulus for three different PBO fibres (data replotted from Ref. [119]. Linear line is a fit to the data predicting a uniform stress band shift rate of 3.7 cm^{-1}/GPa).

Finally, a recent study [124] on heat treated PBO fibres (HM and HM+) has shown that variations (at a spatial resolution of 0.1 μm) in the intensity of layer lines indicate a non-uniform morphology, a factor which contributes to the fact that the fibre modulus does not reach the magnitude of the crystal modulus.

4.3. Crystal deformation in natural fibres

The approaches adopted for highly oriented and crystalline polymer fibres are sufficient to determine the local mechanical properties. However, in the case of semicrystalline and misoriented polymers, such as cellulose, silk, chitin and others, a difficulty exists in the interpretation of results based on seemingly well-intentioned assumptions. In brief, the assumptions of uniform stress and theories of local deformation mechanisms are more difficult to apply when multicomponent and semicrystalline materials are present. In addition to this it must be noted that at low applied stresses, crystal strains will normally increase linearly with fibre stress. However, at higher strains other effects, such as the morphology of the fibres and hydrogen bonding breakdown may influence the form of the deformation. In addition to this, natural polymer fibres tend to be more susceptible to radiation damage in the X-ray beam than synthetic polymers, so particular care must be taken when investigating the materials using a microfocus X-ray beam from a synchrotron source.

The first studies on the crystalline deformation of cellulose using X-ray diffraction were published simultaneously in 1962 [101,102] although only one of these studies was on a native sample [101]. Both studies gave a value of around 130 GPa for the cellulose crystal. These initial studies were followed by an extensive study by Nishino et al. [125] on cellulose polymorphs I, II, III_I, III_{II} and IV_I giving values of 138, 88, 87, 58 and 75 GPa for their respective elastic moduli along the chain direction. A fundamental assumption of this study was that the stress in the crystalline regions was the same as that applied to the samples. This assumption was shown at a later stage to be valid for a range of synthetically produced polyethylenes produced by different methods, where, irrespective of the sample type a value of 235 GPa was obtained [126]. However, this type of assumption was questioned by Becker et al. [127], since experimental values ranging from 17 to 29 GPa were obtained for silk fibres, which were in stark contrast to theoretical determinations.

As already discussed, this assumption of uniform stress may be invalid for *some* polymeric fibres, and certainly cellulosic fibres seem to have more of a series-parallel type structure than a series-type configuration [90]. Nakamae et al. [128] attributed their small experimentally determined value of 23 GPa for the crystal modulus of *Bombyx mori* silk to a 5% shrinkage of the polypeptide chains from a fully extended planar zig–zag conformation, but again one could conceive that in a non-uniform stress situation, the crystal stress is likely to be underestimated, if it is just assumed to be the applied value. Indeed, a recent study by de Oca and Ward [129] has showed for PGA (poly-glycolic acid) crystals that a parallel-series structure might be the best way to represent the deformation of the material, since the theoretical and experimental values of stiffness were so different. Other studies on similar materials to cellulose, such as chitin and chitosan [130] have also shown that seemingly small values of modulus are obtained by these methods, when the uniform stress assumption is applied. Nishino et al. [130] found that α-chitin and chitosan had crystal moduli of 41 GPa and 65 GPa, respectively. These are much lower than values obtained for cellulose, a result that seems strange considering that chitin and cellulose are structurally very similar. It could be that the side chain functionality of chitin changes the conformation of the molecule in chitin, thus reducing its modulus. Nishino et al. [130] carried out identical experiments on chitin when saturated with water and found that the same crystal modulus of 41 GPa was obtained. This result was used to show that the uniform stress model must be valid for these fibres, but again it was assumed prior to the determination of the crystal modulus. It would therefore be interesting to see what value of modulus could be obtained from a non-uniform stress model, such as that proposed by Takayanagi et al. [11].

Other biopolymers have been deformed using the methods developed by Sakurada et al. [102], such as collagen [131]. In this study they found that the chain moduli of a number of samples from various sources ranged from 3–9 GPa. To arrive at these values, Sasaki and Odajima [131] used a quasi-hexagonal packing of chains in the collagen fibrils, a structure that had been postulated from the results of a previous study [132]. An approach like this may be the appropriate method for deriving the true stress–strain curve of cellulosics, and other polymers such as silk, also taking into account the location and proportion of paracrystalline material. Wide-angle X-ray diffraction studies on silk have been performed by Grubb and Jelinski [133], who showed that the crystalline component of the fibres only comprises 12% of the overall structure, with the amorphous component taking up both oriented and misoriented conformations. This may represent the best evidence we have that there are indeed two components of amorphous material in biopolymeric fibres, but more work is required to confirm that the stress is not uniform in such structures. Recently, the shapes of protein segments in collagen-I have been reported, using a small-angle X-ray diffraction technique to derive their three-dimensional topography [134]. Such an approach could be extended to other biopolymers to better understand the relationship between structure and mechanics.

The deformation of cellulose, as revealed by X-ray diffraction, has been used quite extensively to study the structure–property relationships of wood. Wood itself is a biocomposite of fibres (cellulose) and matrix materials (lignin, hemicellulose). The fibres contain a structural feature within their cell walls called the microfibril angle; the angle to the fibre axis at which the cellulose microfibrils (which are of nanoscale proportions in terms of width) are oriented. In this respect, wood can be considered to be a natural nanocomposite. The longitudinal tensile mechanical properties of wood, such as modulus, have long been known to depend intrinsically on the magnitude of the microfibril angle [135]. This angle can be measured using a small-angle X-ray scattering (SAXS) technique [see for example Ref. [136]]. Distinctive streaks corresponding to the microfibrils in the fibre cell walls can be used to accurately measure this parameter. Although SAXS does not determine the detailed properties of the crystal, it is a useful technique for structurally regular semicrystalline natural fibres such as those that comprise wood. A complete review of the work of Fratzl and co-workers is beyond the scope of this article, but they were the first to identify directly that changes in the microfibril angle of wood related directly to mechanical properties using combined *in situ* deformation and SAXS [137]. They have also shown that the macroscopic loss in tensile strength and increase in energy absorption are best compromised with a microfibril angle of 27° [138], and that the cell walls of wood were recovered by a so-called "velcro" mechanism after irreversible deformation [139]. The change in the microfibril angle (μ) with applied tensile strain (ε) was shown to follow a simple linear relationship (Fig. 13). A model for the deformation of the wood was also derived which relied on uniform strain and a critical shear stress between the matrix and fibres. This has certain synergies with misoriented reinforcing phases within

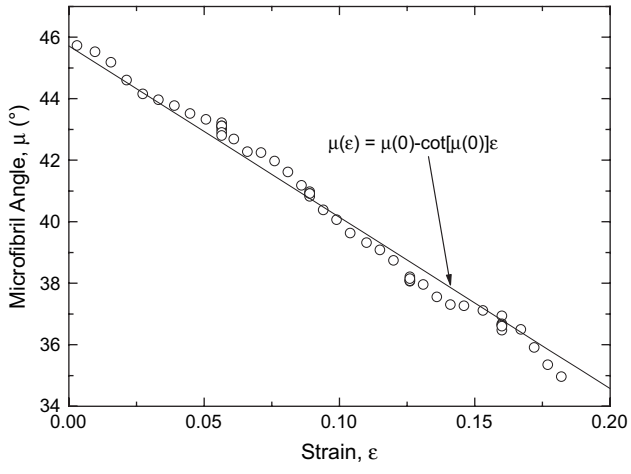

Fig. 13. The change in microfibril angle (μ) of a wet wood foil as a function of tensile strain (ε) as revealed by WAXD (wide-angle X-ray diffraction). Insets show the undeformed and deformed XRD (X-ray diffraction) patterns and the approximate value of the microfibril angle as derived from the integrated intensity around the (002) circle. A linear relationship between microfibril angle ($\mu(\varepsilon) = \mu(0) - \cot[\mu(0)]\varepsilon$) was used to fit the data [139], where $\mu(0)$ is the initial microfibril angle of the specimen (data replotted from Ref. [139]).

polymeric fibres that have a uniform strain type structure, and hence complementary approaches to their deformation could be applied.

Other notable contributions to the understanding of deformation of wood fibres, but using wide-angle X-ray diffraction (WAXD), has been from the recent water absorption–desorption studies of Abe and Yamamoto [140]. They found that the peak positions of the (200) and (004) reflections shifted during desorption, the form of which indicated a lateral expansion of the crystal, indicating that there must be some mechanical interaction between the amorphous matrix constituents of the materials and the fibres. Lateral changes in the crystal dimensions compared to the longitudinal, again using shifts in the 200 and 004 reflections of the WAXD patterns of wood fibres, have recently been shown to indicate local negative Poisson's ratios [141]. Negative values of Poisson's ratio for cellulose fibres have been reported before for cellulose-II [142]. In addition to these effects, it has been shown that the microfibril angle, as derived by SAXS, can decrease after the yield point in the macroscopic deformation of wood fibres [143], a result which has also been seen independently in wet samples of the compressed wood of another species [144].

5. Molecular and fibrous nanocomposites

Discussions will now turn briefly to the deformation micromechanics of fibrous nanocomposites. A full understanding of the local deformation mechanisms in such materials has not yet been achieved within the scientific community, and hence techniques for developing this area are likely to receive significant interest in the near future. Nevertheless some attempts have been made both to determine the interfacial phenomena and to define the laws that govern their properties, for instance, the nanoscale scaling of flaw violations [145].

The work that will be reviewed in this section relates well to the micromechanics and deformation of fibres already discussed. It is now possible to produce nanostructured fibres using electrospinning by the addition of hierarchical pores [146], carbon nanotubes (CNTs) [147] or montmorillonite [148]. The use of CNTs is reminiscent of the ideas first put forward by Takayanagi and his collaborators in 1980; that of a molecular composite [149]. This type of system, where a molecular hard component reinforces a soft polymeric phase, was realised by Takayanagi and others a few years later [150], but only in the form of a film of nylon with phase separated and dispersed chains of P*p*PTA. The principle of such molecular composites (or as has become customary of late, nanocomposites), as outlined by Takayanagi et al. [149], is that the aspect ratio of the rod-like molecules (in this case P*p*PTA [150]) should have a high enough aspect ratio, with the covalent bond between reinforcement and the ''matrix'' material in an ideal state.

It is entirely conceivable, based on the concepts of Takayanagi et al. [149,150] that polymer fibres could be structured in terms of their local orientation to generate the desired mechanical properties by the addition of a second phase. However, one hurdle to overcome is the development of a satisfactory interface, and one way to characterise the efficacy of that property is to use Raman spectroscopy and the other is adequate dispersion, or as stated by Takayanagi et al. [150], phase separation. This degree of dispersion can also be ascertained using Raman spectroscopy, and this will now be discussed.

The concept of a molecular composite, containing diacetylenes, was described explicitly by Lando et al. [151], although much had been done prior to that to characterise their deformation. As already mentioned, Raman band shifts indicating the molecular deformation of polydiacetylene single crystal fibres was the first report of its kind [30]. This was, however, followed a few years later by Galiotis et al. [152] who showed that it was possible to follow the interfacial adhesion between two lap-jointed polydiacetylene fibres made using an epoxy resin adhesive. They found that strong well-defined Raman spectra could be obtained from the fibres and that the strains, as determined by a shift in the polydiacetylene Raman peak, were different in each fibre and within the lap-jointed region [152]. This was the first study to show that it was possible to follow the interface between a fibre and a resin using Raman spectroscopy, but a later paper showed that a shear-lag type stress-transfer occurred over the ends of a fully embedded fibre [153] (Fig. 14). The full details of the number of systems that have been subsequently studied by this method are beyond the scope of this review, and are covered in detail elsewhere [154–156]. It is worth noting that the Takayanagi model [11] has been shown to readily apply to urethane–diacetylene segmented block co-polymers [156]. Block co-polymers are rapidly becoming useful for nanostructuring materials, the progress of which has been reported elsewhere [157]. However, the principle of using Raman spectroscopy to map local deformation in such systems relies on the fact that one can use the local molecular deformation of a fibre or phase, as revealed by the shift in the position of a Raman peak, as a sensor of the local stress state within a composite, provided that the resin used is transparent to the laser or does not interfere spectroscopically with the fibre or phase.

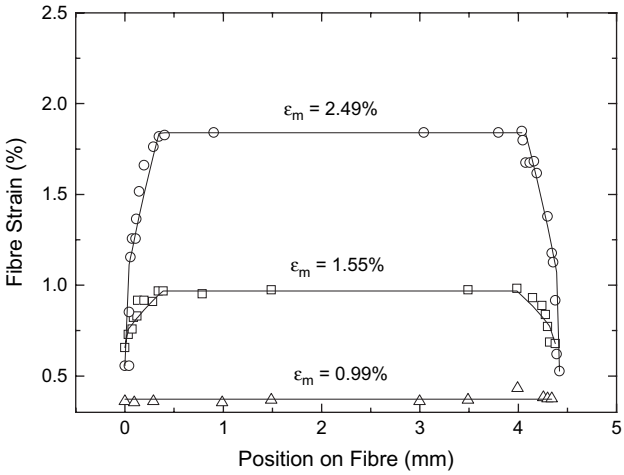

Fig. 14. Axial strain of single poly-1,6-di-(*N*-carbazoyl)-2,4-hexadiene (*p*DCH) fibre as a function of position along the fibre in a model composite at different applied matrix strains (ε_m) (data replotted from Ref. [153]).

After this initial work on a lap-jointed composite [152] other papers were published that showed that local deformation could be followed [158–160] in various forms of molecular composites. To the authors knowledge no other papers have been published which follow the local deformation of two-phase nanocomposites using Raman spectroscopy, other than for CNT systems, which are not within the scope of this article, but recently covered in detail by Wagner and Zhao [161]. In recent times, however, the use of Raman spectroscopy to follow the deformation of natural based nanocomposites has been reported. Before discussing these developments, the production and characterisation of polysaccharide-based (*e.g.* cellulose, chitin and starch) nanocomposites will be reviewed.

The first report on the mechanical properties of a cellulose-based nanocomposite was published in 1995 by Favier et al. [162]. This paper showed that it was possible to isolate rod-like cellulose whiskers, from an edible grade tunicate *Microcosmus sulcatus*, and disperse them in a resin (latex) to make nanocomposites with good reinforcement capability. A great deal of work has been done to generate a number of cellulose nanocomposites by Dufresne et al. [163,164] and Oskman et al. [165] using a variety of sources for the base reinforcement material. Another large development in the field has been the use of bacterial cellulose (from sources such as *Acetobacter xylinum*) for the manufacture of transparent and high-performance composite materials [166,167]. These fibres are produced in culture and so are attractive from an environmental perspective. Since they also have nanometre transverse dimensions they make very attractive materials, not only for composites, but also as support for the growth of cells for tissue engineering applications [168–170]. Here the definitions of ''high-performance'' are best replaced with ''functional'', in that the fibres need to reinforce the generated biomaterial, and eventually a composite material is formed.

Other major developments in the use of natural fibres for composite materials have been the production of all-cellulose composites. The concept was first suggested by Nishino and co-workers [171]. The principle of these materials is to dissolve other cellulose fibres and use that as a matrix which is then reinforced by the intact material. Quite remarkable properties have been obtained for these materials, wherein two-fold increases in the modulus compared to epoxy-cellulose have been observed [172]. All-cellulose nanocomposites have also been produced [173] which also show enhanced properties compared to a composite of two chemically distinct phases. In a similar vein, a group led by Teeri has also developed a method of grafting cellulose fibres to other polymeric materials using XETs (xyloglucan endotransglycosylases) [174]. These are enzymes that under certain conditions can generate glucan chains that can then be grafted to materials such as PMMA (poly-methylmethacrylate). In all these systems the concept of an ''interfaceless composite'', or at least a non-conventional interface, has to be introduced. Little or no information about the nature of such interfaces exists, although some work has been done on following the relative changes in orientation of dissolved cellulose and a reinforcing fibre

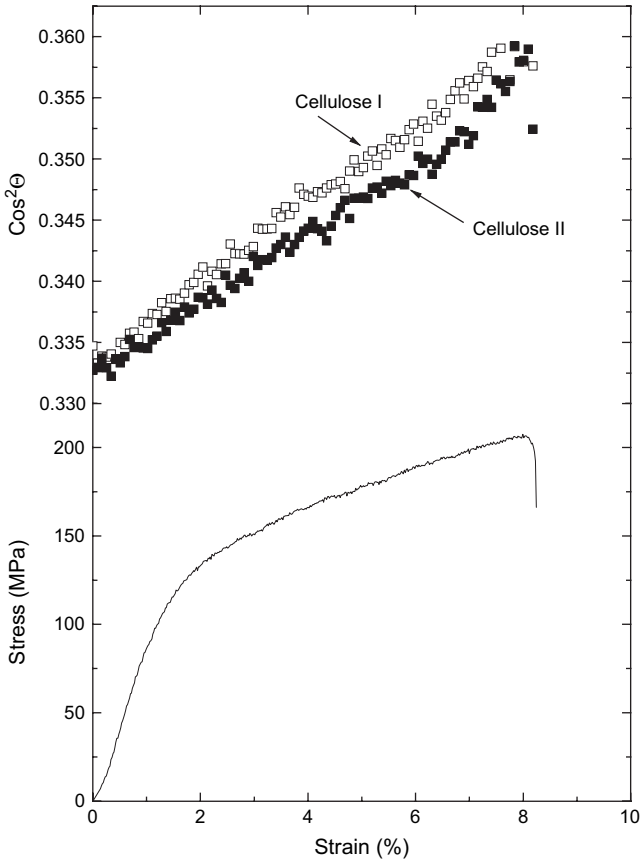

Fig. 15. The change in orientation factor ($\cos^2\theta$) as derived by WAXD measurements as a function of applied strain for an all-cellulose composite (cellulose-I reinforcement with a cellulose-II matrix) and the corresponding stress–strain curve for the material (data reproduced from Ref. [175]).

using X-ray diffraction from a synchrotron source [175]. These data are shown in Fig. 15 [175] and clear differences between the matrix and reinforcement can be seen, with a linear increase in orientation for both. Clearly great advances have been made in developing these materials, where cellulose is grafted with proteins and phases generated by dissolvation and enzymatic catalysis of similar materials, but much needs to be done to better understand the ''interfaces'' that are forming, and how they deform, whether by uniform stress or strain.

6. Conclusions

The development of high-performance fibres for a variety of applications has invigorated research into the understanding of molecular and crystalline orientations, local deformation and morphology. This article has shown both spectroscopy (in particular Raman spectroscopy) and X-ray diffraction (particularly using synchrotron sources) have been critical techniques for our understanding of these concepts. Early developments in these areas showed that it is possible to predict properties of semicrystalline polymers on the basis of stiff crystals embedded in an amorphous matrix, such as in a nanocomposite. However, it is the morphology of this composite

structure that will ultimately determine the mechanical properties. Moreover the location of the amorphous material in relation to the crystals affects whether the structure responds under uniform stress or strain. The early determinations of crystal modulus assumed uniform stress for all polymers. It is clear that a distinction between natural biopolymer-based fibres and those produced by synthetic routes can be made, wherein the former generally appear to have uniform strain type structures and the latter uniform stress. It has been shown that general relationships can be made between physical properties, such as Raman band shift and crystal strain and applied stress and strain, that give a clear signature of whether the structure is a uniform stress or strain type. It is therefore clear that only a combination of these techniques can definitively discriminate such structures. Some materials, such as cellulose, have been shown to have more of a hybrid structure, whereas it is clear that measurements upon silks may have been misinterpreted, with most experimental evidence pointing towards a uniform strain type microstructure.

The effect of crystal orientation has also been reviewed as this plays a critical role in the mechanical properties of high-performance fibres. It has only recently become clear, due to the advances in the spatial resolution of X-ray sources (such as synchrotron), that the skin–core orientation of fibres may play a critical role in mechanical properties. Raman spectroscopy really only looks at an average of crystal and amorphous chain deformations, although some information on molecular orientation can be gleaned. In this sense, with a combination of both techniques, it is possible to obtain a fuller picture of local fibre deformation as a function of both chain deformation and orientation. This enables a test of the uniform stress theories developed for high-performance fibres. For fibres with lower average orientations it is now possible to follow their dominant reorientation processes. Natural fibres, such as cellulose, have been shown to undergo significant reorientation, particularly samples where architecture such as fibril angle is well-defined.

It is worthwhile noting at this point that the relationships derived for both molecular deformation (Raman) and crystal strain (X-ray) shown in Tables 1 and 2 really only apply to the elastic and often initial response of the polymer fibres to deformation. Other key factors play a role at higher levels of deformation, such as hydrogen bonding for instance. It has been shown that hydrogen bonding deformation can be detected using spectroscopic techniques. Non-linearity in the band shift profiles seen with Raman is often the manifestation of such effects, but much more work is required to understand how this relates to the mechanical properties of the fibres, particularly in the presence of water and at elevated temperatures.

Finally, nanocomposites are a subject of wide interest. With the advent of new processing capabilities, such as electrospinning, wherein fibres can be produced with nanoreinforcements built into polymeric structures, it is now possible to engineer new fibres with controlled architectures. Block co-polymers also offer a route for nanostructuring fibres. Needless to say an understanding of how stress is transferred into such structures between the crystalline (hard phase) and matrix materials (soft phase) will again become important and hence the techniques that have been reviewed will also be essential for our understanding of these new classes of materials. Specific examples of where spectroscopic and X-ray techniques might become critical are in following the properties of the interfaces between the matrix and crystals in a nanocomposite fibre. Little is understood about how the nature of an interface in a nanocomposite might differ from that in mesoscale composites, particularly when surface-to-volume ratios increase significantly. Perhaps the next challenge is to take what we know about the effects seen in conventional fibres and to apply not only the techniques used to understand their deformation, but also to test the concepts arising from studying the microstructure of nanocomposite fibres.

Acknowledgements

The authors wish to thank the EPSRC for funding research reported here under grant numbers GR/S44471/01, GR/M82219/01, GR/J68878/01, GR/G09047/01, GR/F06050/01. The authors gratefully acknowledge the provision from Dr. Richard Davies, (ESRF, France), Professor P. Fratzl (Max Planck Institute) and Dr. W. Gindl (BOKU, Austria) for the data used in Figs. 4, 11 and 13, respectively.

References

[1] Treloar LRG. Trans Faraday Soc 1941;37:84–97.
[2] Kolsky H, Shearman AC. Proc Phys Soc 1943;55:383–95.
[3] Crawford SM, Kolsky H. Proc Phys Soc B 1951;64:119–25.
[4] Crawford SM, Kolsky H. Proc Phys Soc A 1951;64:215.
[5] Hermans PH. Physics and chemistry of cellulose fibres. London: Elsevier Publishing Company; 1949.
[6] Ward IM. Proc Phys Soc 1962;80:1176–88.
[7] Patterson D, Ward IM. Trans Faraday Soc 1957;53:1516–26.
[8] Halpin JC, Kardos JL. J Appl Phys 1972;43:2235–41.
[9] Harris B. Engineering composite materials. IOM Communications Ltd.; 1999.
[10] Northolt MG, vanderHout R. Polymer 1985;26:310–6.
[11] Takayanagi M, Imada K, Kajiyama T. J Polym Sci C 1966;15:263.
[12] Young RJ. J Text Inst 1995;86:360–81.
[13] Raman CV, Krishnan KS. Nature 1928;121:501–2.
[14] Steinfeld JI. Molecules and radiation: an introduction to molecular spectroscopy. Cambridge, Massachussets and London: MIT Press; 1979.
[15] Liang CY, Krimm S, Sutherland GBBM. J Chem Phys 1956;25:543–8.
[16] Liang CY, Krimm S, Sutherland GBBM. J Chem Phys 1956;25:549–62.
[17] Liang CY, Krimm S. J Chem Phys 1956;25:563–71.
[18] Krimm S, Liang CY. J Polym Sci 1956;22:95–112.
[19] Krimm S, Liang CY, Sutherland GBBM. J Polym Sci 1956;22:227–47.
[20] Palm A. J Phys Chem 1951;55:1320–4.
[21] Flaugh PL, O'Donnell SE, Asher SA. Appl Spectrosc 1984;38:847–50.
[22] Delhaye M, Dhamelincourt P. J Raman Spectrosc 1975;3:33–43.
[23] Zhurkov SN, Novak II, Vettegren VI. Dokl Akad Nauk SSSR 1964;157:1431–5.
[24] Zhurkov SN, Korsukov VI, Novak II. Infrared spectroscopic study of the chemical bonds in stressed polymers, Fracture 1979. In: Proceedings of the second international conference on fracture; 1979. p. 545–50.
[25] Roylance DK, deVries KL. J Polym Sci Polym Lett Ed 1971;9:443–7.
[26] Evans RA, Hallam HE. Polymer 1976;17:838–9.

[27] Cunningham A, Ward IM, Willis HA, Zichy V. Polymer 1974;15:749–56.
[28] Wool RP. J Appl Polym Sci Polym Phys Ed 1975;13:1795–808.
[29] Wool RP. Polym Eng Sci 1980;20:805–15.
[30] Mitra VK, Risen WM, Baughman RH. J Chem Phys 1977;66:2731–6.
[31] Badger RM. J Chem Phys 1934;2:128–31.
[32] Batchelder DN, Bloor D. J Polym Sci Polym Phys Ed 1979;17:569–81.
[33] Young RJ, Bloor D, Batchelder DN, Hubble CL. J Mater Sci 1978;13:62–71.
[34] Galiotis C. PhD thesis, University of London; 1982.
[35] Penn L, Milanovich F. Polymer 1979;20:31–6.
[36] Galiotis C, Robinson IM, Young RJ, Smith BJE, Batchelder DN. Polym Commun 1985;26:354–5.
[37] Edwards HGM, Hakiki S. Br Polym J 1989;21:505–12.
[38] Young RJ, Lu D, Day RJ. Polym Int 1991;24:71–6.
[39] Day RJ, Robinson IM, Zakikhani M, Young RJ. Polymer 1987;28:1833–40.
[40] Shen DY, Hsu SL. Polymer 1982;23:969–73.
[41] Prasad K, Grubb DT. J Polym Sci B Polym Phys Ed 1989;27:381–403.
[42] Kip BJ, van Eijk CP, Meier RJ. J Polym Sci B Polym Phys Ed 1991;29:99–108.
[43] Young RJ, Day RJ, Zakikhani M. J Mater Sci 1990;25:127–36.
[44] Yeh W-Y, Young RJ. Polymer 1999;40:857–70.
[45] Yeh W-Y, Young RJ. J Macromol Sci Phys 1998;B37:83–118.
[46] Northolt MG, Baltussen JJM, Schaffers-Korff B. Polymer 1995;36:3485–92.
[47] Zhang H, Davies GR, Ward IM. Polymer 1992;33:2651–8.
[48] Kong K, Eichhorn SJ. J Macromol Sci Phys 2005;44:1123–6.
[49] Kitagawa T, Yabuki K, Young RJ. Polymer 2001;42:2101–12.
[50] Kitagawa T, Yabuki K, Young RJ. J Macromol Sci Phys 2002;42:61–76.
[51] Young RJ, Lu D, Day RJ, Knoff WF, Davis HA. J Mater Sci 1992;27:5431–40.
[52] Bollas D, Parthenios J, Galiotis C. Phys Rev B 2006;73:094103.
[53] Blackwell J, Vasko PD, Koenig JL. J Appl Phys 1970;41:4375–9.
[54] Ellis J, Bath J. J Am Chem Soc 1940;62:2859–61.
[55] Liang CY, Marchessault RH. J Polym Sci 1959;37:385–95.
[56] Liang CY, Marchessault RH. J Polym Sci 1959;39:269–78.
[57] Marchessault RH, Liang CY. J Polym Sci 1960;43:71–84.
[58] Lin VJC, Koenig JL. Bull Am Phys Soc 1975;20:372.
[59] Wiley JH, Atalla RH. Carbohydr Res 1987;160:113–29.
[60] Pemberton JE, Sobocinski RL. J Am Chem Soc 1989;11:432–4.
[61] Edwards HGM, Farwell DW, Webster D. Spectrochim Acta A 1997;53:2383–92.
[62] Edwards HGM, Farwell DW. J Raman Spectrosc 1995;26:901–9.
[63] Hogg LJ, Edwards HGM, Farwell DW, Peters AT. J Soc Dyers Colour 1994;110:196–9.
[64] Akhtar W, Edwards HGM, Farwell DW, Nutbrown M. Spectrochim Acta A 1997;53:1021–31.
[65] Hamad WY, Eichhorn S. ASME J Eng Mat Tech 1997;119:309–13.
[66] Eichhorn SJ, Hughes M, Snell R, Mott L. J Mat Sci Lett 2000;19:721–3.
[67] Eichhorn SJ, Sirichaisit J, Young RJ. J Mater Sci 2001;36:3129–35.
[68] Eichhorn SJ, Young RJ. Cellulose 2001;8:197–207.
[69] Fischer S, Schenzel K, Fischer K, Diepenbrock W. Macromol Symp 2005;223:41–56.
[70] Peetla P, Schenzel K, Diepenbrock W. Appl Spectrosc 2006;60:682–91.
[71] Gierlinger N, Schwanniger M, Reinecke A, Burgert I. Biomacromolecules 2006;7:2077–81.
[72] Hinterstoisser B, Salmén L. Cellulose 1999;6:251–63.
[73] Åkerholm M, Hinterstoisser B, Salmén L. Carbohydr Res 2004;339:569–78.
[74] Langan P, Nishiyama Y, Chanzy H. J Am Chem Soc 1999;121:9940–6.
[75] Langan P, Nishiyama Y, Chanzy H. Biomacromolecules 2001;2:410–6.
[76] Nishiyama Y, Langan P, Chanzy H. J Am Chem Soc 2002;124:9074–82.
[77] Nishiyama Y, Sugiyama J, Chanzy H, Langan P. J Am Chem Soc 2003;125:14300–6.
[78] Jarvis M. Nature 2003;426:611–2.
[79] Wang YN, Galiotis C, Bader DL. J Biomech 2000;33:483–6.
[80] Sirichaisit J, Young RJ, Vollrath F. Polymer 2000;41:1223–7.
[81] Sirichaisit J, Brookes VL, Young RJ, Vollrath F. Biomacromolecules 2003;4:387–94.
[82] Termonia Y. Macromolecules 1994;27:7378–81.
[83] O'Brien JP, Fahnestock SR, Termonia Y, Gardner KH. Adv Mater 1998;10:1185–95.
[84] Stephens JS, Fahnestock SR, Farmer RS, Kiick KL, Chase DB, Rabolt JF. Biomacromolecules 2005;6:1405–13.
[85] Brookes VL. PhD thesis, University of Manchester Institute of Science and Technology; 2005.
[86] Sinsawat A, Putthanarat S, Magoshi Y, Pachter R, Eby RK. Polymer 2002;43:1323–30.
[87] Sinsawat A, Putthanarat S, Magoshi Y, Pachter R, Eby RK. Polymer 2003;44:909–10.
[88] Tashiro K. Prog Polym Sci 1993;18:377–435.
[89] Brookes VL, Young RJ, Vollrath F. Biomacromolecules, submitted for publication.
[90] Eichhorn SJ, Young RJ, Davies GR. Biomacromolecules 2005;6:507–13.
[91] Kitagawa T, Tashiro K, Yabuki K. J Polym Sci Part B Polym Phys 2002;40:1269–80.
[92] Kitagawa T, Tashiro K, Yabuki K. J Polym Sci Part B Polym Phys 2002;40:1281–7.
[93] Cael JJ, Gardner KH, Koenig JL, Blackwell J. J Chem Phys 1975;62:1145–53.
[94] Sturcova A, Davies GR, Eichhorn SJ. Biomacromolecules 2005;6:1055–61.
[95] Meyer KH, Lotmar W. Helv Chim Acta 1936;19:68–86.
[96] Meyer KH, Lotmar W. Helv Chim Acta 1937;20:232–44.
[97] Lyons WJ. J Appl Phys 1959;30:796–7.
[98] Treloar LRG. Polymer 1960;1:290–303.
[99] Treloar LRG. Polymer 1960;1:95–103.
[100] Treloar LRG. Polymer 1960;1:279–89.
[101] Mann J, Roldan-Gonzalez L. Polymer 1962;3:549–53.
[102] Sakurada I, Nukushina Y, Ito T. J Polym Sci 1962;57:651–60.
[103] Peterlin A. Kolloid Z Z Polym 1967;216:129.
[104] Mark RE, Kaloni PE, Tang RC, Gillis PP. Science 1969;164:72–3.
[105] Manley RSJ. Nature 1964;204:1155–7.
[106] Jakeways R, Ward IM, Wilding MA, Hall IH, Desborough IJ, Pass MG. J Polym Sci Polym Phys Ed 1975;13:799–813.
[107] Ciferri A, Ward IM, editors. Ultra high modulus polymers. Essex, UK: Applied Science Publishers; 1979.
[108] Northolt MG, vanAarts JJ. J Polym Sci Polym Lett Ed 1973;11:333–57.
[109] Gardner KH, English AD, Forsyth VT. Macromolecules 2004;37:9654–6.
[110] Northolt MG. Polymer 1980;21:1199–204.
[111] Nakamae K, Nishino T, Shinizu Y, Matsumoto T. Polym J 1987;19:451–9.
[112] Wolfe JF, Sybert PD, Sybert JR. US Patent 4 533 693, 1985.
[113] Krause SJ, Haddock TB, Vezie DL, Lenhert PG, Hwang WF, Price GE, et al. Polymer 1988;29:1354–64.
[114] Martin DC, Thomas EL. Macromolecules 1991;24:2450–60.
[115] Tashiro K, Yoshino J, Kitagawa T, Murase H, Yabuki K. Macromolecules 1998;31:5430–40.
[116] Nakamae K, Nishino T, Gotoh Y, Matsui R, Nagura M. Polymer 1999;40:4629–34.
[117] Engström P, Fiedler S, Riekel C. Rev Sci Instrum 1995;66:1348–50.
[118] Riekel C, Dieing, Engström P, Vincze L, Martin C, Mahendrasingam A. Macromolecules 1999;32:7859–65.
[119] Davies RJ, Montes-Morán, Riekel C, Young RJ. J Mater Sci 2001;36:3079–87.
[120] Montes-Morán MA, Davies RJ, Riekel C, Young RJ. Polymer 2002;43:5219–26.
[121] Davies RJ, Montes-Morán, Riekel C, Young RJ. J Mater Sci 2003;38:2105–15.
[122] Davies RJ, Eichhorn SJ, Riekel C, Young RJ. Polymer 2004;45:7693–704.

[123] Davies RJ, Eichhorn SJ, Riekel C, Young RJ. Polymer 2005;46:1935–42.
[124] Davies RJ, Burghammer M, Riekel C. Macromolecules 2005;38:3364–70.
[125] Nishino T, Takano K, Nakamae K. J Polym Sci Part B Polym Phys 1995;33:1647–51.
[126] Nakamae K, Nishino T, Ohkubo H. J Macromol Sci Phys 1991;30:1–23.
[127] Becker MA, Mahoney DV, Lenhert PG, Eby RK, Kaplan D, Adams WW. ACS Symp Ser 1994;544:185–95.
[128] Nakamae K, Nishino T, Ohkubo H. Polymer 1989;30:1243–6.
[129] de Oca HM, Ward IM. Polymer 2006;47:7070–7.
[130] Nishino T, Matsui R, Nakamae K. J Polym Sci Part B Polym Phys 1999;37:1191–6.
[131] Sasaki N, Odajima S. J Biomech 1996;29:655–8.
[132] Hulmes JDS, Miller A. Nature 1979;282:878–80.
[133] Grubb DT, Jelinski LW. Macromolecules 1997;30:2860–7.
[134] Orgel JPRO, Irving TC, Miller A, Wess TJ. Proc Natl Acad Sci USA 2006;103:9001–5.
[135] Cave ID. Wood Sci Technol 1969;3:40–8.
[136] Reiterer A, Jakob HF, Stanzl-Tschegg SE, Fratzl P. Wood Sci Technol 1998;32:335–45.
[137] Reiterer A, Lichtenegger H, Tschegg S, Fratzl P. Philos Mag A 1999;79:2173–84.
[138] Reiterer A, Lichtenegger H, Fratzl P, Stanzl-Tschegg SE. J Mater Sci 2001;36:4681–6.
[139] Keckes J, Burgert I, Fruhmann K, Muller M, Kolln K, Hamilton M, et al. Nat Mater 2003;2:810–4.
[140] Abe K, Yamamoto H. J Wood Sci 2005;51:334–8.
[141] Peura M, Grotkopp I, Lemke H, Vikkula A, Laine J, Muller M, et al. Biomacromolecules 2006;7:1521–8.
[142] Nakamura K, Wada M, Kuga S, Okano T. J Polym Sci B Polym Phys Ed 2004;42:1206–11.
[143] Kolln K, Grotkopp I, Burghammer M, Roth SV, Funari SS, Dommach M, et al. J Synchrotron Radiat 2005;12:739–44.
[144] Kamiyama T, Suzuki H, Sugiyama J. J Struct Biol 2005;151:1–11.
[145] Gao HJ, Ji BH, Jager IL, Arzt E, Fratzl P. Proc Natl Acad Sci USA 2003;100:5597–600.
[146] Bognitzki M, Czado W, Frese T, Schaper A, Hellwig M, Steinhart M, et al. Adv Mater 2001;13:70–2.
[147] Ko F, Gogotsi Y, Ali A, Naguib N, Ye H, Yang G, et al. Adv Mater 2003;15:1161–5.
[148] Fong H, Liu WD, Wang CS, Vaia RA. Polymer 2002;43:775–80.
[149] Takayanagi M, Ogata T, Morikawa M, Kai T. J Macromol Sci Phys 1980;17:591–615.
[150] Ueta S, Sakamoto T, Takayanagi M. Polym J 1993;25:31–40.
[151] Angkaew S, Wang H-Y, Lando JB. Chem Mater 1994;6:1444–51.
[152] Galiotis C, Young RJ, Batchelder DN. J Mater Sci Lett 1983;2:263–6.
[153] Galiotis C, Young RJ, Yeung PHJ, Batchelder DN. J Mater Sci 1984;19:3640–8.
[154] Schadler LS, Galiotis C. Int Mater Rev 1995;40:116–34.
[155] Andrews MC, Young RJ. J Raman Spectrosc 1993;24:539–44.
[156] Stanford JL, Young RJ, Day RJ. Polymer 1991;32:1713.
[157] Hamley IW. Nanotechnology 2003;14:39.
[158] Hu X, Stanford JL, Young RJ. Polymer 1994;35:80–5.
[159] Casado R, Lovell PA, Stanford JL, Young RJ. Macromol Symp 1997;118:395–400.
[160] Young RJ, Day RJ, Ang PP. Polym Commun 1990;31:47–9.
[161] Zhao Q, Wagner HD. Philos Trans R Soc London Ser A 2004;362:2407–24.
[162] Favier V, Chanzy H, Cavaille JY. Macromolecules 1995;28:6365–7.
[163] Eichhorn SJ, Baillie CA, Zafeiropoulos N, Mwaikambo LY, Ansell MP, Dufresne A, et al. J Mater Sci 2001;36:2107–31.
[164] Samir MASA, Alloin F, Dufresne A. Biomacromolecules 2005;6:612–26.
[165] Kvien I, Tanem BS, Oksman K. Biomacromolecules 2005;6:3160–5.
[166] Yano H, Sugiyama J, Nakagaito AN, Nogi M, Matsuura T, Hikita M, et al. Adv Mater 2005;17:153–5.
[167] Dufresne A. Compos Interfaces 2000;7:53–67.
[168] Svensson A, Nicklasson E, Harrah T, Panilaitis B, Kaplan DL, Brittberg M, et al. Biomaterials 2005;26:419–31.
[169] Backdahl H, Helenius G, Bodin A, Nannmark U, Johansson BR, Risberg B, et al. Biomaterials 2006;27:2141–9.
[170] Bodin A, Gustafsson L, Gatenholm P. J Biomater Sci Polym Ed 2006;17:435–47.
[171] Nishino T, Matsuda I, Hirao K. Macromolecules 2004;37:7683–7.
[172] Gindl W, Schoberl T, Keckes J. Appl Phys A 2006;83:19–22.
[173] Gindl W, Keckes J. Polymer 2005;46:10221–5.
[174] Zhou Q, Greffe L, Baumann MJ, Malmstrom E, Teeri TT, Brumer H. Macromolecules 2005;38:3547–9.
[175] Gindl W, Martinschitz KJ, Boesecke P, Keckes J. Compos Sci Technol 2006;66:2639–47.

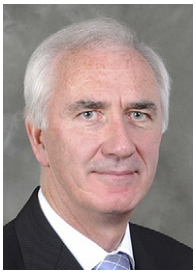

Professor Robert J. Young FREng, Head of the School of Materials – University of Manchester, UK. Professor Young was born in 1948. He studied Natural Sciences at the University of Cambridge, and gained a B.A. in 1969 and a Ph.D. (1973), after which he obtained a Research Fellowship at St. John's College, Cambridge. In 1975 he took up a Lectureship in Materials Science at Queen Mary College, London. He became Professor of Polymer Science and Technology in Manchester in 1986, a position which he still holds. During the same year he served as Head of the Department of Polymer Science and Technology, before taking up the role of Head of Manchester Materials Science Centre in 1987. From 1992 to 1997 he was the Royal Society Wolfson Research Professor of Material Science. Professor Young also chaired the Metallurgy and Materials panels for the UK Research Assessment Exercises in 1996 and 2001. In 2004 he was appointed Head of the School of Materials in the newly formed University of Manchester.

Professor Young's main research interest is the relationships between structure and properties in polymers and composites, publishing over 250 papers and a number of books. His research has been supported by the EPSRC, industry and the European Union and his interests have extended recently to the field nanotechnology. He has lectured extensively on the public understanding of science at the Royal Society (Zeneca Lecture), the British Association (Royal Society Lecture) and for a number of other organisations. He was elected as a Fellow of the Royal Academy of Engineering in 2006.

Dr. Stephen J. Eichhorn, Senior Lecturer in Polymer Physics and Biomaterials – University of Manchester, UK. Dr. Eichhorn was born in 1972 and studied his first degree in Physics at Leeds (B.Sc., 1993), a Masters at Bangor/University of Manchester (1995) and a Ph.D. at the University of Manchester (1999). He was appointed as a lecturer in Materials Science in 2002 and was promoted to Senior Lecturer in 2006.

Dr. Eichhorn's main research interest is the relationships between structure and properties in polymers and composites, with particular emphasis on natural materials. He has focussed mainly on cellulosic fibres and composites, with particular interests in using Raman spectroscopy to map local deformation. His research has been supported by the EPSRC, Nuffield Foundation and the Royal Society. He is a member of the American Chemical Society and is the membership secretary for the Cellulose and Renewable Materials division. Dr. Eichhorn has given numerous talks at international conferences, including ACS National Meetings and a Gordon research conference on "The Chemistry of Polysaccharides". He has also, since joining the School of Materials, given talks to schoolchildren as part of a widening participation and liaison programme. Dr. Eichhorn is also a member of the Institute of Physics.